PEDIATRICS INTERNATIONAL Official Journal of the Japan Pediatric Society

Involvement of brain structures in childhood epilepsy with centrotemporal spikes

Journal:	*Pediatrics International*
Manuscript ID	PED-00542-2021.R1
Manuscript Type:	Original Articles
Date Submitted by the Author:	n/a
Complete List of Authors:	Ito, Yuji; Aichi Prefecture Mikawa Aoitori Medical and Rehabilitation Center for Developmental Disabilities, Pediatrics; Nagoya University Graduate School of Medicine, Pediatrics Maki, Yuki; Nagoya University Graduate School of Medicine, Pediatrics Okai, Yu ; Nagoya University, Department of Pediatrics Kidokoro, Hiroyuki; Nagoya university , Pediatrics Bagarinao, Epifanio; Nagoya University, Brain & Mind Research Center Takeuchi, Tomoya; Japanese Red Cross Nagoya First Hospital, Department of Neurology, Children's Medical Center Ohno, Atsuko; Toyota Municipal Child Development Center, Pediatric Neurology Nakata, Tomohiko; Nagoya Daigaku, Pediatrics Ishihara, Naoko; Fujita Hoken Eisei Daigaku, Pediatrics Okumura, Akihisa; Aichi Medical University, Pediatrics Yamamoto, Hiroyuki; Nagoya University Graduate School of Medicine, Pediatrics Maesawa, Satoshi; Nagoya University, Brain & Mind Research Center Natsume, Jun; Nagoya University Graduate School of Medicine, Department of Pediatrics
Keywords:	Benign epilepsy with centrotemporal spikes (BECTS), basal ganglia, Childhood epilepsy with centrotemporal spikes (CECTS), cingulate gyrus, EEG-fMRI

Involvement of brain structures in childhood epilepsy with centrotemporal spikes

Yuji Ito, MD, PhD[a, b, c], Yuki Maki, MD[a, b], Yu Okai, MD[a, b, d], Hiroyuki Kidokoro, MD, PhD[a, b], Epifanio Bagarinao, PhD[a], Tomoya Takeuchi, MD, PhD[e], Atsuko Ohno, MD[d], Tomohiko Nakata, MD, PhD[b], Naoko Ishihara, MD, PhD[f], Akihisa Okumura, MD, PhD[g], Hiroyuki Yamamoto, MD, PhD[a, b], Satoshi Maesawa, MD, PhD[a, h], Jun Natsume, MD, PhD[a, b, i]

[a] Brain & Mind Research Center, Nagoya University, Aichi, Japan

[b] Department of Pediatrics, Nagoya University Graduate School of Medicine, Aichi, Japan

[c] Department of Pediatrics, Aichi Prefecture Mikawa Aoitori Medical and Rehabilitation Center for Developmental Disabilities, Aichi, Japan

[d] Department of Pediatric Neurology, Toyota Municipal Child Development Center, Aichi, Japan

[e] Department of Pediatrics, Japanese Red Cross Nagoya Daiichi Hospital, Aichi, Japan

[f] Department of Pediatrics, Fujita Health University School of Medicine, Aichi, Japan

[g] Department of Pediatrics, Aichi Medical University, Aichi, Japan

[h] Department of Neurosurgery, Nagoya University Graduate School of Medicine, Aichi, Japan

[i] Department of Developmental Disability Medicine, Nagoya University Graduate School of Medicine, Aichi, Japan

Address correspondence to: Yuji Ito, MD, PhD

Brain & Mind Research Center, Nagoya University

65 Tsurumai-cho, Showa-ku, Nagoya, Aichi 466-8550, Japan

Phone: (+81) 52-744-1975; Fax: (+81) 52-731-8131

E-mail: yuji.ito@med.nagoya-u.ac.jp

Running title: EEG-fMRI analysis in CECTS

Category of manuscript: Original Articles

Number of text pages: 25

Number of words: 3133

Number of references: 32

Number of tables: 2

Number of figures: 3

Abstract

Background

We aimed to investigate electroencephalography (EEG)-functional magnetic resonance imaging (fMRI) findings to elucidate the interictal epileptiform discharge (IED)-related functional alterations in deep brain structures as well as the neocortex in childhood epilepsy with centrotemporal spikes (CECTS).

Methods

Ten children with CECTS (median age; 8.2 years) referred to our hospital within a year of onset were eligible for inclusion. They underwent EEG-fMRI recording during sleep. In addition, longitudinal evaluations, including medical examinations, intelligence tests, and questionnaires about developmental disabilities, were performed. The initial evaluation was performed at the same time as the EEG-fMRI, and the second evaluation was performed over 2 years after the initial evaluation.

Results

Three children were unable to maintain sleep during the EEG-fMRI recording, and the remaining seven children were eligible for further assessment. All patients showed unilateral-dominant centrotemporal spikes during scans. One patient had only positive hemodynamic responses, while the others had both positive and negative hemodynamic responses. All patients showed IED-related hemodynamic responses in the bilateral neocortex. For deep brain structures, IED-related hemodynamic responses were observed in the cingulate gyrus (n=4), basal ganglia (n=3), thalamus (n=2), and default mode network (n=1). Seizure frequencies at the second evaluation were infrequent or absent, and the longitudinal results of intelligence tests and questionnaires were within normal ranges.

Conclusions

We demonstrated that IEDs affect broad brain areas, including deep brain structures such as cingulate gyrus, basal ganglia, and thalamus. Deep brain structures may play an important role in the pathophysiology of CECTS.

Keywords: Benign epilepsy with centrotemporal spikes (BECTS), basal ganglia, Childhood epilepsy with centrotemporal spikes (CECTS), cingulate gyrus, EEG-fMRI

1. Introduction

Childhood epilepsy with centrotemporal spikes (CECTS) is the most common epilepsy syndrome affecting children, accounting for about 15% of pediatric epilepsy cases [1]. The etiology of CECTS is not fully elucidated, and mutations in some genes, including *GRIN2A*, are reported to cause CECTS [2]. Although patients with CECTS have been regarded as having good intellectual and seizure prognosis, there is a tendency toward intellectual disabilities and poor seizure outcomes in cases of atypical benign partial epilepsy or epilepsy with continuous spikes and waves during slow-wave sleep [3]. In addition, it has been suggested that at least 10 to 20% of patients with CECTS exhibit language or attention-deficit hyperactivity disorders, even if their intelligence quotient is within the normal range [4, 5].

Recently, several studies have used resting-state functional magnetic resonance imaging (fMRI) to clarify the mechanisms underlying the behavioral and cognitive comorbidities in CECTS. Children with CECTS and interictal epileptiform discharges (IEDs) show decreased functional connectivity in the default mode network, the core region of which is the posterior cingulate gyrus, and they have an atypical language network and reduced sensorimotor connectivity [6, 7]. In addition, children with CECTS show an increased amplitude of low-frequency fluctuation in the thalamus, which positively correlates with the number of IEDs during scans [8]. Decreased amplitude of low-frequency fluctuation is also observed in the anterior cingulate cortex, putamen, and caudate, and similar findings in the basal ganglia positively correlate with verbal intelligence quotient [9]. From the above, it is clear the functional alterations occurring in broad brain areas including deep brain structures such as the cingulate gyrus, basal ganglia, thalamus. However, whether IEDs affect the functional alterations

and neuropsychological outcomes needs to be further examined using other neurophysiological imaging modalities.

Electroencephalography (EEG)-fMRI combines the strengths of EEG (high temporal resolution) and fMRI (high spatial resolution), and it can be used to evaluate neural activity in the whole brain, including deep brain structures [10, 11]. In addition, EEG-fMRI can be used to evaluate functional abnormalities relevant to IEDs by detecting changes in cerebral blood flow, visualized as blood oxygen level-dependent (BOLD) signals [10, 11]. In previous EEG-fMRI analyses of CECTS, the distribution of IED-related BOLD signals was shown to vary from person to person. They were also found to appear in the pericentral and perisylvian gyri as well as the premotor and prefrontal cortices [12, 13]. However, the distribution of IED-related BOLD signals in deep brain structures has not been clarified.

Therefore, the aim of this study was to investigate the EEG-fMRI findings in deep brain structures, such as the cingulate gyrus, basal ganglia, and thalamus as well as in the neocortex including perisylvian areas, to elucidate the IED-related functional alterations of broad brain areas in CECTS. Our hypothesis is that children with CECTS have IED-related BOLD signals in the cingulate gyrus, basal ganglia, and thalamus.

2. Material and methods

2.1. Ethics Statement

This study was conducted in accordance with the Declaration of Helsinki and was approved by the research ethics board of Nagoya University Graduate School of Medicine. All parents provided written informed consent for their child's participation in the study, and written informed assent was obtained from school-aged children. The

manuscript was prepared in accordance with STrengthening the Reporting of OBservational studies in Epidemiology (STROBE) guidelines.

2.2. Study Population

Between August 2015 and October 2017, a total of ten children with CECTS who were referred to our hospital within a year of the seizure onset for further examination and treatment were eligible for inclusion. All patients consented to participate in this study and underwent EEG-fMRI recordings during sleep. They also underwent longitudinal medical examinations by pediatric neurologists and intelligence tests by clinical psychologists in order to understand the course of the disease. Their parents responded to questionnaires related to developmental disabilities to document the status of the patients longitudinally. The initial evaluation was performed at the same time as EEG-fMRI recordings. The second evaluation was carried out more than 2 years after the initial evaluation.

2.3. EEG-fMRI Acquisition

The MRI data were obtained at the Brain and Mind Research Center of Nagoya University, using a Siemens Magnetom Verio 3-Tesla magnetic resonance (MR) scanner (Siemens, Erlangen, Germany) with a 32-channel head coil. High-resolution T1-weighted images were acquired using a three-dimensional magnetization-prepared rapid gradient-echo acquisition sequences with the following imaging parameters: repetition time, 2.5 s; echo time, 2.48 ms; 192 sagittal slices with a distance factor of 50% and 1-mm thickness; in-plane voxel resolution, 1 mm × 1 mm; field of view, 256 mm × 256 mm; and matrix dimension, 256 × 256. fMRIs were recorded in a single continuous session for 15 min using a T2-weighted gradient-echoplanar imaging

sequence with the following imaging parameters: repetition time, 2.5 s; echo time, 30 ms; field of view, 192 mm; matrix dimension, 64 × 64; 39 transverse slices with a 0.5 mm inter-slice interval and 3 mm thickness; flip angle, 80 degrees; and a total of 360 volumes.

Simultaneous EEG and electrocardiogram during fMRI were continuously recorded inside the MR scanner using an MR-compatible recording system (Electrical Geodesics Incorporated, Eugene, OR, USA). A 32-channel sensor-net EEG cap connected to a combined digitizer-amplifier system was worn by the children during the recordings. The data from the amplifier were sampled at 1 kHz and were continuously transmitted using NetStation version 5.0 software (Electrical Geodesics Incorporated) [14]. Children were sedated to a soporific drug-induced sleep state using triclofos sodium syrup at 80 mg per kg body weight. Foam pads were also used to minimize head motion and children's discomfort.

2.4. EEG and fMRI Preprocessing

The raw EEG data were preprocessed using NetStation version 5.0 software. Gradient artifacts were eliminated using the template subtraction method, and the ballistocardiogram artifact was eliminated using principal component analysis [15, 16]. Two trained pediatric neurologists (YI, YM) independently marked the start points in the rising phase of spikes according to both morphology and spatial distribution, which were similar to those recorded outside the MR scanner using the same equipment prior to the scan. Only the onsets of spikes for which the two neurologists agreed were used for subsequent analysis.

fMRI data were preprocessed using SPM version 12 software (Welcome Trust Center for Neuroimaging, London, UK) running on MATLAB (MathWorks, Natick,

MA, USA). The initial 5 volumes were excluded to account for the initial BOLD signal instability at the beginning of the scan. The remaining volumes were corrected for temporal differences in slice acquisition and head movement, spatially normalized to the standard Montreal Neurological Institute space, and smoothed using an isotropic three-dimensional Gaussian kernel of 8 mm full width at half maximum.

2.5. Event-Related EEG-fMRI Analysis

Event-related EEG-fMRI analysis was performed using an in-house MATLAB script and SPM 12 software. Identified IED onsets were marked to generate a series of spikes, which were then convolved with four hemodynamic response functions (HRFs) peaking at 3, 5, 7, and 9 seconds [17]. The HRFs represented the hemodynamic responses after the neural activities, such as IEDs. All regressors were used in the statistical analysis using a general linear model approach [18]. A statistical t-map was created for each regressor using the other regressors as confounders. A combined t-map was constructed by taking the most significant t-value from the four t-maps based on the four HRFs at each voxel. This combined t-map was used for subsequent analysis. Concerning the significance level, a hemodynamic response required five contiguous voxels having a t-value > 3.1, consistent with $p < .05$, corrected for multiple comparisons (family-wise error rate) according to the number of voxels using the four HRFs [17]. Combined t-maps were superimposed onto individual co-registered T1-weighted images. We evaluated the significant IED-related BOLD signals in neocortex including perisylvian areas and deep brain structures such as the cingulate gyrus, basal ganglia, and thalamus, in addition to the location of the global maximum t-value.

2.6. Cognitive and Behavioral Outcomes

Cognitive and behavioral outcomes were evaluated using the Japanese versions of the Wechsler Intelligence Scale for Children, Fourth Edition (WISC-IV), the Autism-Spectrum Quotient children's version (AQ-Child), and attention-deficit hyperactivity disorder rating scale (ADHD-RS). The WISC-IV was used to calculate the full-scale intelligence quotient and four index scores consisting of the verbal comprehensive index, perceptual reasoning index, working memory index, and processing speed index for children over 5 years old [19]. The Tanaka-Binet Intelligence Scale V (Taken Publishing, Tokyo, Japan) was used to calculate the intelligence quotient for children under 5 years of age. The AQ-Child was completed by the parents for the screening of autism-spectrum disorder, and more than 25 points indicated a high risk of autism-spectrum disorder [20]. The ADHD-RS was completed by the parents for the screening of attention-deficit hyperactivity disorder. Inattentive scores (0–27 points), hyperactive/impulsive scores (0–27 points), and total scores (0–54 points) were calculated, and higher scores indicated more severe attention-deficit hyperactivity disorder traits [21].

3. Results

EEG-fMRI was performed in ten children with CECTS. Three children were unable to maintain sleep during the scan and were therefore excluded from further analyses. Only the data from the remaining seven children were used for subsequent analyses.

The clinical characteristics of the seven children with CECTS are shown in Table 1. Median ages at the initial and second evaluations were 8 years and 2 months, and 11 years and 0 months, respectively. Seizure types in all patients were Sylvian seizures, which are typically characterized by focal motor seizures starting unilaterally from the face while asleep. In the second evaluation, seizures were infrequent, and no child

converted to either atypical benign partial epilepsy or epilepsy with continuous spikes and waves during slow sleep. With regard to past medical history, patient 2 had a simple febrile seizure at the age of 1 year and 6 months. No patient had a family history of convulsive disorders, including epilepsy. Patient 6 showed an arachnoid cyst in the temporal lobe on MRI. The results of the WISC-IV, including the full-scale intelligence quotient and four index scores, the AQ-Child, and the ADHD-RS were within normal ranges in all patients. At the initial evaluation, the intelligence quotient of patient 1 was 115 using the Tanaka-Binet Intelligence Scale V, which was suitable for his age, and patient 7 did not take the intelligence test.

EEG-fMRI findings in children with CECTS are shown in Table 2. During scans, all patients showed unilateral-dominant centrotemporal spikes, which are typical for CECTS (Figure 1A, 2A), and no patient experienced a seizure during the scan. Patient 1 had only positive BOLD responses, and the other patients had both positive and negative BOLD responses. All patients had significant IED-related BOLD responses bilaterally in the neocortical regions. For perisylvian areas, 4 patients had significant bilateral IED-related BOLD responses and 2 had significant unilateral IED-related BOLD responses ipsilateral to the IEDs. For deep brain structures, significant IED-related hemodynamic responses were observed in the cingulate gyrus (n=4), basal ganglia (n=3), and thalamus (n=2). Patient 4 had significant IED-related hemodynamic responses in the bilateral cingulate gyrus, basal ganglia, and thalamus (Figure 1B). Patient 5 had significant IED-related hemodynamic responses in the default mode network, including the posterior cingulate gyrus (Figure 2B). EEG-fMRI findings in the other patients are shown in Figure 3.

4. Discussion

In this EEG-fMRI study using the multiple HRF method, we documented the distribution of IED-related BOLD signals in deep brain structures as well as the neocortex in children with CECTS. In terms of the hypothesis, significant IED-related BOLD signals in the cingulate gyrus and basal ganglia were often observed in CECTS. Significant IED-related hemodynamic responses were also observed in the thalamus and the default mode network. These results suggest that the broad brain areas including deep brain structures play an important role in the pathophysiology of CECTS.

The most important finding of this study using the multiple HRF method is that IED-related BOLD signals in the cingulate gyrus and basal ganglia were often observed in children with CECTS. This result differs from previous EEG-fMRI studies, which showed IED-related BOLD responses mainly in the cerebral neocortex, specifically in the frontal and parietal lobes [12, 13]. This difference could be due to the use of the canonical HRF as implemented in the SPM software in previous studies. Although canonical HRF has been commonly used in EEG-fMRI studies, it has been reported that the transition of BOLD signal changes in children with CECTS was different from that of canonical HRF. The average peak of BOLD responses related to the centrotemporal spikes was found to occur before that of the canonical HRF, and the beginning of BOLD signal changes was observed before the onset of spikes [22]. Furthermore, the BOLD response could also vary across brain regions, subjects, and sessions. Therefore, the canonical HRF may not sufficiently account for these variabilities [10, 17]. For these reasons, the multiple HRF method used in this study could better capture the variations in the BOLD signals, resulting in the detection of significant IED-related hemodynamic responses in the deep brain structures.

The present results demonstrated that there are significant IED-related BOLD signals in the anterior and/or posterior cingulate gyri in more than half of the children

with CECTS. The anterior cingulate gyrus is mainly involved in emotional and cognitive functions such as attention, cognitive control, working memory, set maintenance, and goal-directed behavior [23]. The dysfunction of the anterior cingulate gyrus has been reported in various psychiatric conditions, such as obsessive-compulsive disorder and depression [23]. Whereas the posterior cingulate gyrus is mainly involved in the maintenance of stable brain activities by regulating the attentional focus, and the dysfunction of the posterior cingulate gyrus has been observed in some developmental disabilities, including autism spectrum disorder and attention deficit hyperactivity disorder [24]. The posterior cingulate gyrus is also involved in supporting internally directed conditions by playing a central role in the default mode network [24]. The default mode network is one of the main brain networks active at rest, which affects cognitive function [25]. Previous EEG-fMRI studies in epilepsy patients showed that the activation and deactivation of the default mode network might cause cognitive impairments [26, 27, 28]. Children with CECTS are at high risk of developing cognitive and behavioral symptoms [4, 5], which might be explained by the IED-related functional alterations in the anterior and posterior cingulate gyri.

In this study, we also reported that IED-related BOLD signals were observed in the basal ganglia and thalamus in children with CECTS. IED-related functional alterations in these structures were also identified in the previous EEG-fMRI studies of atypical benign partial epilepsy, and epilepsy with continuous spikes and waves during slow-wave sleep, which occasionally converted from CECTS, was likely to demonstrate significant IED-related BOLD signals in broader brain areas than did CECTS [12, 13, 28, 29]. The group analysis of ten patients with atypical benign partial epilepsy revealed significant IED-related BOLD signals in the thalamus [29]. The group analysis of 12 children with epilepsy with continuous spikes and waves during slow-wave sleep

demonstrated significant IED-related BOLD signals in the thalamus and basal ganglia, suggesting a contribution to the pathological synchronization and propagation of epileptic activities followed by secondary cognitive impairment [28]. Recently, CECTS, atypical benign partial epilepsy, and epilepsy with continuous spikes and waves during slow-wave sleep has been regarded as a single continuum of epileptic disorders that have different entities [2]. Therefore, the similarity of the IED-related BOLD signal distribution in the thalamus and basal ganglia in these three epilepsy syndromes could support their unification.

Most children with CECTS in this study had IED-related BOLD signals in the perisylvian areas, which is consistent with previous EEG-fMRI studies on CECTS [12, 13]. The perisylvian areas include the Broca and Wernicke areas, which play an important role in language function. The most common language disabilities in children with CECTS are language comprehension and word generation [30]. It has been suggested that language disabilities appear early in the onset of CECTS and that longer duration of epilepsy is more likely to impair language function [31, 32]. Persistent IED-related functional alterations in perisylvian areas might be the underlying cause of language disabilities in this population.

This study has several limitations. First, the sample size was small, and the results of the intelligence tests and questionnaires were within normal ranges in all children. More study participants will be needed to clarify the relationship between the distribution patterns of IED-related BOLD signals in the deep brain structures and neuropsychological outcomes. Second, most children took antiepileptic drugs during the evaluations, which might have affected the EEG-fMRI findings. Third, the intelligence quotient of one child was not scaled at the initial evaluation. Fourth, there were no patients with CECTS showing atypical evolution between the initial and second

evaluations. Therefore, in this study, we could not detect the key findings underlying the atypical evolution using EEG-fMRI. Finally, it would be beneficial to compare EEG-fMRI findings with other neuroimaging modalities such as MRI volumetry, diffusion tensor imaging, and resting-state functional MRI. A multimodal neuroimaging study is needed to clarify the pathophysiology of CECTS in more detail.

5. Conclusions

The present study using EEG-fMRI demonstrated several IED-related functional alterations of broad brain areas, including deep brain structures, such as the cingulate gyrus, basal ganglia, and thalamus in children with CECTS. These results emphasize the important role of deep brain structures in the pathophysiology of CECTS.

Acknowledgments

This research was supported by The Japan Epilepsy Research Foundation with project title “Prediction of cognitive outcome using EEG-fMRI in early stage of benign childhood epilepsy with centrotemporal spikes (Principal investigator: Yuji Ito)”. The funders had no role in the study design, data collection, analysis and interpretation of the data, or preparation of the manuscript.

We would like to acknowledge Mr. Akira Ishizuka (radiological technologist) for his technical support during the MRI scans and Editage (www.editage.com) for English language editing.

Conflict of Interest Disclosure

Jun Natsume belongs to the Department of Developmental Disability Medicine in Nagoya University Graduate School of Medicine, which is the laboratory endowed by

Aichi Prefecture. The remaining authors declare no competing interests concerning the materials or methods used in this study or the findings specified in this paper.

Author contributions

Conception and design: IY, KH, and NJ. Acquisition of data: IY, MY, OY, TT, OA, NT, IN, OA, and NJ. Analysis and interpretation of data: IY, MY, OY, KH, BE, YH, MS, and NJ. Drafting of the article: IY. Critically revising the article: MY, OY, KH, BE, TT, OA, NT, IN, OA, YH, MS, and NJ. All authors have read and approved the final manuscript.

References

1. Proposal for revised classification of epilepsies and epileptic syndromes. Commission on Classification and Terminology of the International League Against Epilepsy. *Epilepsia.* 1989; 30: 389-99.
2. Lesca G, Moller RS, Rudolf G, Hirsch E, Hjalgrim H, Szepetowski P. Update on the genetics of the epilepsy-aphasia spectrum and role of GRIN2A mutations. *Epileptic. Disord.* 2019; 21: 41-7.
3. Doose H, Hahn A, Neubauer BA, Pistohl J, Stephani U. Atypical "benign" partial epilepsy of childhood or pseudo-lennox syndrome. Part II: family study. *Neuropediatrics*. 2001; 32: 9-13.
4. Jurkeviciene G, Endziniene M, Laukiene I, et al. Association of language dysfunction and age of onset of benign epilepsy with centrotemporal spikes in children. *Eur. J. Paediatr. Neurol.* 2012; 16: 653-61.
5. Kim EH, Yum MS, Kim HW, Ko TS. Attention-deficit/hyperactivity disorder and attention impairment in children with benign childhood epilepsy with centrotemporal spikes. *Epilepsy. Behav.* 2014; 37: 54-8.
6. Bear JJ, Chapman KE, Tregellas JR. The epileptic network and cognition: What functional connectivity is teaching us about the childhood epilepsies. *Epilepsia*. 2019; 60: 1491-507.
7. Xiao F, An D, Lei D, et al. Real-time effects of centrotemporal spikes on cognition in rolandic epilepsy: An EEG-fMRI study. *Neurology*. 2016; 86: 544-51.
8. Zhu Y, Yu Y, Shinkareva SV, et al. Intrinsic brain activity as a diagnostic biomarker in children with benign epilepsy with centrotemporal spikes. *Hum. Brain. Mapp.* 2015; 36: 3878-89.

9. Wu Y, Ji GJ, Zang YF, et al. Local activity and causal connectivity in children with benign epilepsy with centrotemporal spikes. *PLoS. One*. 2015; 10: e0134361.

10. Gotman J. Epileptic networks studied with EEG-fMRI. *Epilepsia*. 2008; 49 Suppl 3: 42-51.

11. Ito Y, Maesawa S, Bagarinao E, et al. Subsecond EEG-fMRI analysis for presurgical evaluation in focal epilepsy. *J. Neurosurg.* 2020. DOI: 10.3171/2020.1.jns192567

12. Boor R, Jacobs J, Hinzmann A, et al. Combined spike-related functional MRI and multiple source analysis in the non-invasive spike localization of benign rolandic epilepsy. *Clin. Neurophysiol.* 2007; 118: 901-9.

13. Lengler U, Kafadar I, Neubauer BA, Krakow K. fMRI correlates of interictal epileptic activity in patients with idiopathic benign focal epilepsy of childhood. A simultaneous EEG-functional MRI study. *Epilepsy. Res.* 2007; 75: 29-38.

14. Mandelkow H, Halder P, Boesiger P, Brandeis D. Synchronization facilitates removal of MRI artefacts from concurrent EEG recordings and increases usable bandwidth. *Neuroimage*. 2006; 32: 1120-6.

15. Allen PJ, Josephs O, Turner R. A method for removing imaging artifact from continuous EEG recorded during functional MRI. *Neuroimage.* 2000; 12: 230-9.

16. Niazy RK, Beckmann CF, Iannetti GD, Brady JM, Smith SM. Removal of fMRI environment artifacts from EEG data using optimal basis sets. *Neuroimage.* 2005; 28: 720-37.

17. Bagshaw AP, Aghakhani Y, Benar CG, et al. EEG-fMRI of focal epileptic spikes: analysis with multiple haemodynamic functions and comparison with gadolinium-enhanced MR angiograms. *Hum. Brain. Mapp.* 2004; 22: 179-92.

18. Al-Asmi A, Benar CG, Gross DW, et al. fMRI activation in continuous and spike-triggered EEG-fMRI studies of epileptic spikes. *Epilepsia*. 2003; 44: 1328-39.

19. Wechsler D. *Wechsler Intelligence Scale for Children*, 4th edn. The Psychological Corporation, San Antonio, Texas, 2003.

20. Wakabayashi A, Baron-Cohen S, Uchiyama T, et al. The autism-spectrum quotient (AQ) children's version in Japan: a cross-cultural comparison. *J. Autism. Dev. Disord.* 2007; 37: 491-500.

21. Zhang S, Faries DE, Vowles M, Michelson D. ADHD Rating Scale IV: psychometric properties from a multinational study as a clinician-administered instrument. *Int. J. Methods. Psychiatr. Res.* 2005; 14: 186-201.

22. Masterton RA, Harvey AS, Archer JS, et al. Focal epileptiform spikes do not show a canonical BOLD response in patients with benign rolandic epilepsy (BECTS). *Neuroimage*. 2010; 51: 252-60.

23. Gasquoine PG. Localization of function in anterior cingulate cortex: from psychosurgery to functional neuroimaging. *Neurosci. Biobehav. Rev.* 2013; 37: 340-48.

24. Leech R, Sharp DJ. The role of the posterior cingulate cortex in cognition and disease. *Brain*. 2014; 137: 12-32.

25. Raichle ME, Mintun MA. Brain work and brain imaging. *Annu. Rev. Neurosci.* 2006; 29: 449-76.

26. Archer JS, Warren AE, Stagnitti MR, Masterton RA, Abbott DF, Jackson GD. Lennox-Gastaut syndrome and phenotype: secondary network epilepsies. *Epilepsia.* 2014; 55: 1245-54.

27. Gotman J, Grova C, Bagshaw A, Kobayashi E, Aghakhani Y, Dubeau F. Generalized epileptic discharges show thalamocortical activation and suspension of the default state of the brain. *Proc. Natl. Acad. Sci. U S A.* 2005; 102: 15236-40.

28. Siniatchkin M, Groening K, Moehring J, et al. Neuronal networks in children with continuous spikes and waves during slow sleep. *Brain*. 2010; 133: 2798-813.

29. Moeller F, Moehring J, Ick I, et al. EEG-fMRI in atypical benign partial epilepsy. *Epilepsia.* 2013; 54: e103-8.

30. Teixeira J, Santos ME. Language skills in children with benign childhood epilepsy with centrotemporal spikes: A systematic review. *Epilepsy. Behav.* 2018; 84: 15-21.

31. Vannest J, Tenney JR, Gelineau-Morel R, Maloney T, Glauser TA. Cognitive and behavioral outcomes in benign childhood epilepsy with centrotemporal spikes. *Epilepsy. Behav.* 2015; 45: 85-91.

32. Teixeira JM, Santos ME, Oom P. Oral language in children with benign childhood epilepsy with centrotemporal spikes. *Epilepsy. Behav.* 2020; 111: 107328.

Table 1. Clinical characteristics of children with childhood epilepsy with centrotemporal spikes

Patient /Sex	Age at onset of epilepsy	Initial evaluation												Second evaluation									
		Age	AED	Seizure frequency	WISC-Ⅳ					AQ-Child	ADHD-RS			Age	AED	Seizure frequency	WISC-Ⅳ					AQ-Child	ADHD-RS		
					FSIQ	VCI	PRI	WMI	PSI		Total	IA	HI				FSIQ	VCI	PRI	WMI	PSI		Total	IA	HI
1/M	3y8m	4y4m	LEV	monthly	N/A*					15	6	3	3	6y9m	LEV	monthly	102	97	104	126	83	11	0	0	0
2/M	7y0m	7y8m	CBZ	monthly	101	78	98	126	113	24	3	1	2	10y0m	CBZ	yearly	132	129	115	141	107	15	3	3	0
3/F	7y3m	8y1m	CLB	monthly	122	140	115	106	96	11	2	1	1	11y6m	CBZ	yearly	135	131	127	120	124	7	0	0	0
4/F	7y4m	8y10m	CBZ	yearly	83	86	72	85	104	4	0	0	0	11y0m	CBZ	None	93	103	91	85	96	4	0	0	0
5/M	8y0m	8y2m	None	yearly	118	97	124	123	110	10	2	0	2	10y6m	None	None	122	105	127	133	102	15	1	1	0
6/M	10y4m	10y11m	CBZ	weekly	111	99	113	100	121	14	0	0	0	13y4m	CBZ	None	108	101	100	106	121	9	0	0	0
7/F	11y1m	11y10m	None	yearly	N/A					10	2	0	2	13y10m	None	None	108	103	113	120	88	18	1	1	0

*The intelligence quotient of patient 1 was 115 using the Tanaka-Binet Intelligence Scale V, which was suitable for his age.

ADHD-RS, Attention-Deficit Hyperactivity Rating Scale; AED, antiepileptic drugs; AQ-Child, Autism-Spectrum Quotient, Children' s version; CBZ, carbamazepine; CLB, clobazam; F, female; FSIQ, full-scale intelligence quotient; m, months; HI, hyperactive/impulsive; IA, inattentive; LEV, levetiracetam; M, male; N/A, not available; PRI, perceptual reasoning index; PSI, processing speed index; VCI, verbal comprehensive index; WISC-IV, Wechsler Intelligence Scale for Children, Fourth Edition; WMI, working memory index; y, years.

Table 2. EEG-fMRI findings in children with childhood epilepsy with centrotemporal spikes

			EEG-fMRI findings (peak location, t-value)				
Patient	Type of IEDs	No of IEDs	Global maximum	Perisylvian area	Cingulate gyrus	Basal ganglia	Thalamus
1	R-F Sp	32	L-S-O gyrus, 5.01	R-insula, 4.10	R-middle-C gyrus, 3.55	L-caudate, 4.32	L-thalamus, 3.41
2	L-F Sp	20	L-postcentral gyrus, -4.98	L-Rolandic operculum, -3.61	None	None	None
3	R-FT Sp	17	R-fusiform gyrus, -4.54	R-M-T gyrus, -3.72	L-posterior-C gyrus, -3.74	None	None
4	L-FP Sp	330	L-posterior-C gyrus, 11.46	L-S-T gyrus, -3.76	L-posterior-C gyrus, 11.46	R-putamen, 4.47	R-thalamus, 3.35
5	L-PT Sp	50	L-S-F gyrus, -6.10	L-Rolandic operculum, -5.22	R-anterior-C gyrus, -4.79	None	None
6	L-FT Sp	20	L-postcentral gyrus, 4.36	L-Rolandic operculum, 3.85	None	L-caudate, -3.41	None
7	R-FT Sp	40	R-postcentral gyrus, -4.15	None	None	None	None

C, cingulate; EEG-fMRI, electroencephalography-fMRI; F, frontal; I, inferior; IED, interictal epileptiform discharge; L, left; M, middle; N/A, not available; O, occipital; P, parietal; R, right; S, superior; Sp, spike; T, temporal.

Figure legends

Figure 1. A girl with significant interictal epileptiform discharge (IED)-related blood oxygen level-dependent (BOLD) responses in the bilateral cingulate gyrus, basal ganglia, and thalamus using event-related electroencephalography (EEG)-functional magnetic resonance imaging (fMRI) analysis.

Patient 4 is an 8-year-old female with childhood epilepsy and centrotemporal spikes.

(A) During fMRI recording, EEG shows repetitive C3/P3 spikes (red outline).

(B) The EEG-fMRI findings reveal the left posterior cingulate gyrus to be the peak location of the global maximum t-value (t=11.46, Montreal Neurological Institute space coordinate: [x, y, z] = [-12, -20, 40], yellow arrow). Among the deep brain structures, the bilateral cingulate gyrus, basal ganglia, and thalamus show significant IED-related positive BOLD responses.

The significance level is set using a threshold t-value of 3.1 for positive BOLD response and -3.1 for negative BOLD response, consistent with $p < .05$, and corrected for multiple comparisons (family-wise error rate) using the multiple hemodynamic response function method.

Figure 2. A boy with significant interictal epileptiform discharge (IED)-related blood oxygen level-dependent (BOLD) responses in the default mode network using event-related electroencephalography (EEG)-functional magnetic resonance imaging (fMRI) analysis.

Patient 5 is an 8-year-old male with childhood epilepsy with centrotemporal spikes.

(A) During fMRI recording at the initial evaluation, EEG shows frequent P3/T5 spikes (red outline).

(B) The EEG-fMRI findings reveal the left superior frontal gyrus as the site of the global maximum t-value (t=-6.10, Montreal Neurological Institute space coordinate: [x, y, z] = [-16, -2, 72], yellow arrow). For deep brain structures, significant IED-related positive BOLD responses are observed in the default mode network, including the posterior cingulate gyrus. A significant IED-related negative BOLD response is observed in the anterior cingulate gyrus.

The significance level is set using a threshold t-value of 3.1 for positive BOLD response and -3.1 for negative BOLD response, consistent with $p < .05$, and corrected for multiple comparisons (family-wise error rate) using the multiple hemodynamic response function method.

Figure 3. Five children with significant interictal epileptiform discharge (IED)-related blood oxygen level-dependent (BOLD) responses using event-related electroencephalography (EEG)-functional magnetic resonance imaging (fMRI) analysis.

(A) Patient 1 is a 4-year-old male with childhood epilepsy and centrotemporal spikes. The EEG-fMRI findings reveal the left superior occipital gyrus to be the peak location of the global maximum t-value (t=5.01, Montreal Neurological Institute space coordinate: [x, y, z] = [-22, -66, 26], yellow arrow). Among the deep brain structures, the cingulate gyrus, basal ganglia, and thalamus show significant IED-related positive BOLD responses.

(B) Patient 2 is a 7-year-old male with childhood epilepsy and centrotemporal spikes. The EEG-fMRI findings reveal the left postcentral gyrus to be the peak location of the global maximum t-value (t=-4.98, Montreal Neurological Institute space coordinate: [x, y, z] = [-52, -24, 26], yellow arrow).

(C) Patient 3 is an 8-year-old female with childhood epilepsy and centrotemporal spikes. The EEG-fMRI findings reveal the right fusiform gyrus to be the peak location of the global maximum t-value (t=-4.54, Montreal Neurological Institute space coordinate: [x, y, z] = [44, -58, -16], yellow arrow). Among the deep brain structures, the cingulate gyrus shows significant IED-related negative BOLD responses.

(D) Patient 6 is a 10-year-old male with childhood epilepsy and centrotemporal spikes. The EEG-fMRI findings reveal the left postcentral gyrus to be the peak location of the global maximum t-value (t=4.36, Montreal Neurological Institute space coordinate: [x, y, z] = [-36, -36, 70], yellow arrow). Among the deep brain structures, the basal ganglia show significant IED-related negative BOLD responses.

(E) Patient 7 is an 11-year-old female with childhood epilepsy and centrotemporal spikes. The EEG-fMRI findings reveal the right postcentral gyrus to be the peak location of the global maximum t-value (t=-4.15, Montreal Neurological Institute space coordinate: [x, y, z] = [24, -40, 44], yellow arrow).

The significance level is set using a threshold t-value of 3.1 for positive BOLD response and -3.1 for negative BOLD response, consistent with $p < .05$, and corrected for multiple comparisons (family-wise error rate) using the multiple hemodynamic response function method.

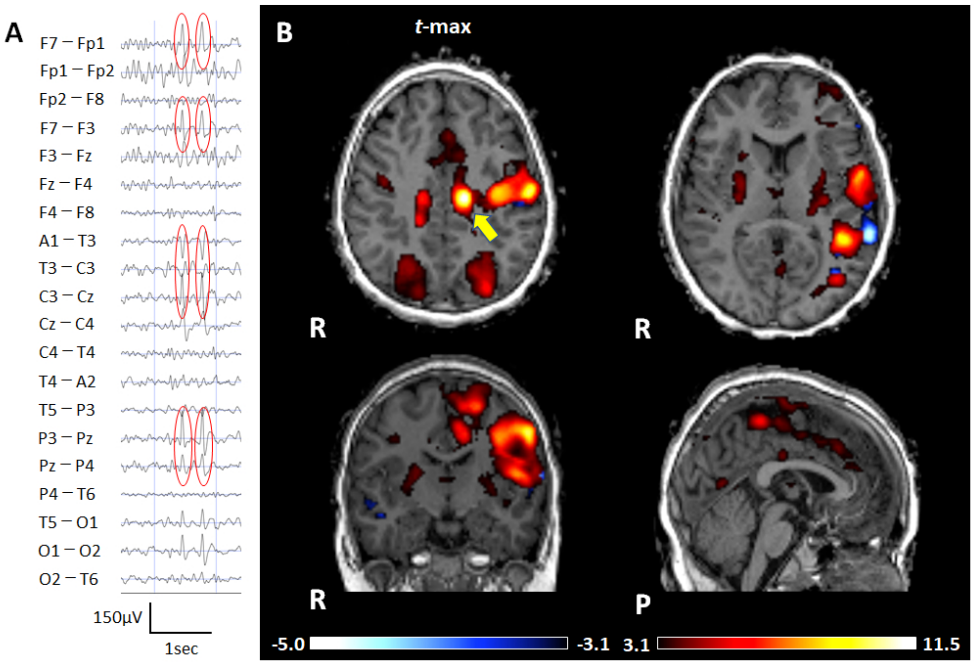

Figure 1. A girl with significant interictal epileptiform discharge (IED)-related blood oxygen level-dependent (BOLD) responses in the bilateral cingulate gyrus, basal ganglia, and thalamus using event-related electroencephalography (EEG)-functional magnetic resonance imaging (fMRI) analysis.
Patient 4 is an 8-year-old female with childhood epilepsy and centrotemporal spikes.
(A) During fMRI recording, EEG shows repetitive C3/P3 spikes (red outline).
(B) The EEG-fMRI findings reveal the left posterior cingulate gyrus to be the peak location of the global maximum t-value (t=11.46, Montreal Neurological Institute space coordinate: [x, y, z] = [-12, -20, 40], yellow arrow). Among the deep brain structures, the bilateral cingulate gyrus, basal ganglia, and thalamus show significant IED-related positive BOLD responses.
The significance level is set using a threshold t-value of 3.1 for positive BOLD response and -3.1 for negative BOLD response, consistent with $p < .05$, corrected for multiple comparisons (family-wise error rate) using the multiple hemodynamic response function method.

86x57mm (300 x 300 DPI)

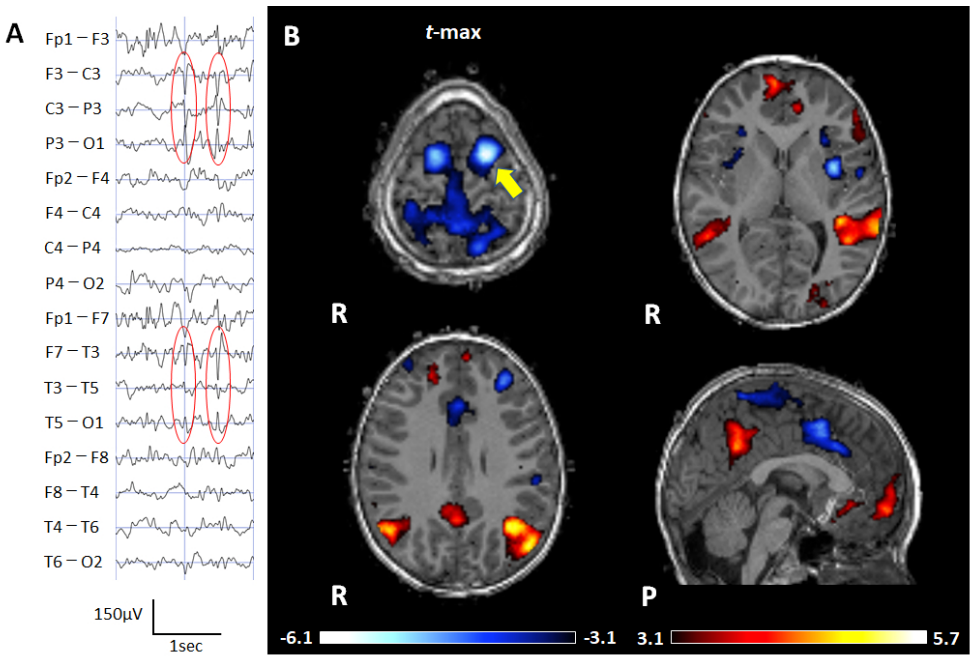

Figure 2. A boy with significant interictal epileptiform discharge (IED)-related blood oxygen level-dependent (BOLD) responses in the default mode network using event-related electroencephalography (EEG)-functional magnetic resonance imaging (fMRI) analysis.
Patient 5 is an 8-year-old male with childhood epilepsy with centrotemporal spikes.
(A) During fMRI recording at the initial evaluation, EEG shows frequent P3/T5 spikes (red outline).
(B) The EEG-fMRI findings reveal the left superior frontal gyrus as the site of the global maximum t-value (t=-6.10, Montreal Neurological Institute space coordinate: [x, y, z] = [-16, -2, 72], yellow arrow). For deep brain structures, significant IED-related positive BOLD responses are observed in the default mode network, including the posterior cingulate gyrus. A significant IED-related negative BOLD response is observed in the anterior cingulate gyrus.
The significance level is set using a threshold t-value of 3.1 for positive BOLD response and -3.1 for negative BOLD response, consistent with $p < .05$, corrected for multiple comparisons (family-wise error rate) using the multiple hemodynamic response function method.

87x57mm (300 x 300 DPI)

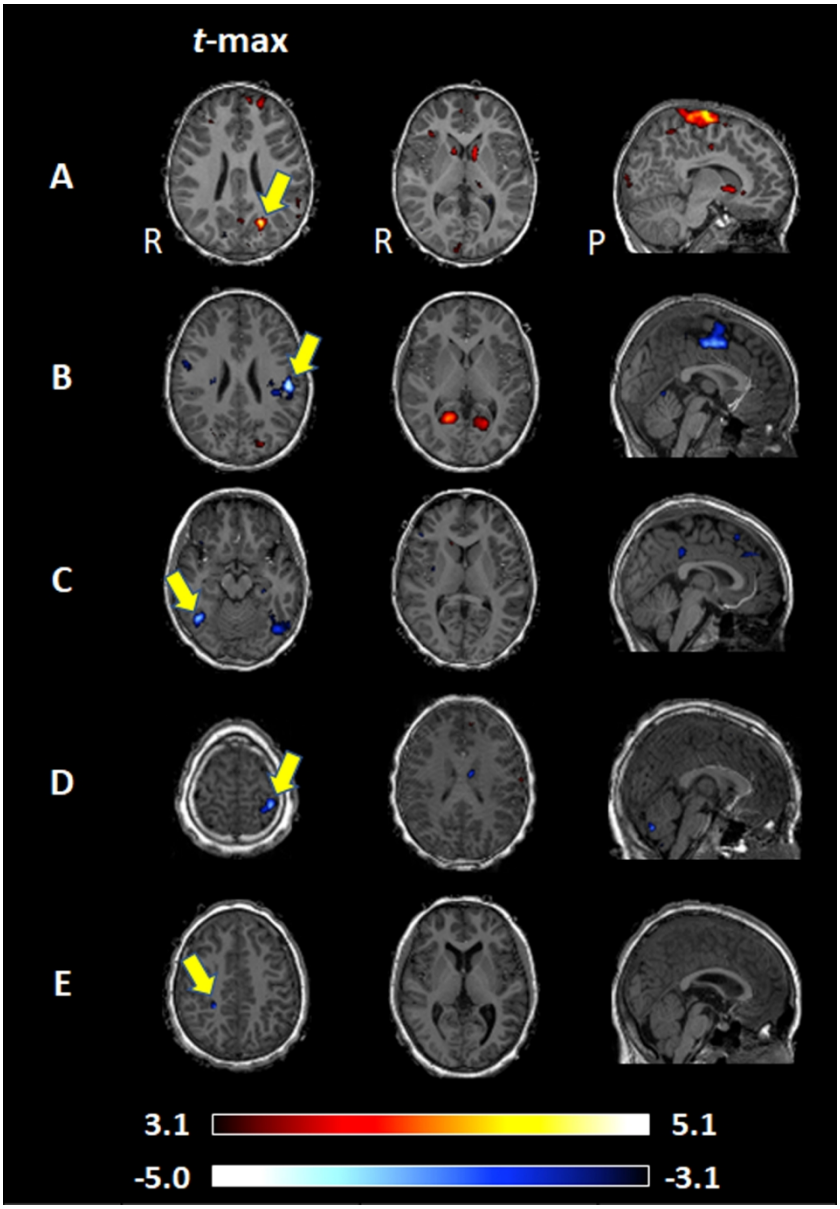

Figure 3. Five children with significant interictal epileptiform discharge (IED)-related blood oxygen level-dependent (BOLD) responses using event-related electroencephalography (EEG)-functional magnetic resonance imaging (fMRI) analysis.

(A) Patient 1 is a 4-year-old male with childhood epilepsy and centrotemporal spikes. The EEG-fMRI findings reveal the left superior occipital gyrus to be the peak location of the global maximum t-value (t=5.01, Montreal Neurological Institute space coordinate: [x, y, z] = [-22, -66, 26], yellow arrow). Among the deep brain structures, the cingulate gyrus, basal ganglia, and thalamus show significant IED-related positive BOLD responses.

(B) Patient 2 is a 7-year-old male with childhood epilepsy and centrotemporal spikes. The EEG-fMRI findings reveal the left postcentral gyrus to be the peak location of the global maximum t-value (t=-4.98, Montreal Neurological Institute space coordinate: [x, y, z] = [-52, -24, 26], yellow arrow).

(C) Patient 3 is an 8-year-old female with childhood epilepsy and centrotemporal spikes. The EEG-fMRI findings reveal the right fusiform gyrus to be the peak location of the global maximum t-value (t=-4.54, Montreal Neurological Institute space coordinate: [x, y, z] = [44, -58, -16], yellow arrow). Among the deep

brain structures, the cingulate gyrus shows significant IED-related negative BOLD responses. (D) Patient 6 is a 10-year-old male with childhood epilepsy and centrotemporal spikes. The EEG-fMRI findings reveal the left postcentral gyrus to be the peak location of the global maximum t-value (t=4.36, Montreal Neurological Institute space coordinate: [x, y, z] = [-36, -36, 70], yellow arrow). Among the deep brain structures, the basal ganglia show significant IED-related negative BOLD responses. (E) Patient 7 is an 11-year-old female with childhood epilepsy and centrotemporal spikes. The EEG-fMRI findings reveal the right postcentral gyrus to be the peak location of the global maximum t-value (t=-4.15, Montreal Neurological Institute space coordinate: [x, y, z] = [24, -40, 44], yellow arrow). The significance level is set using a threshold t-value of 3.1 for positive BOLD response and -3.1 for negative BOLD response, consistent with $p < .05$, and corrected for multiple comparisons (family-wise error rate) using the multiple hemodynamic response function method.

127x183mm (300 x 300 DPI)